Simultaneous three-dimensional inversion of large-scale AEM data for changeability and conductivity using the GEMTIP model and moving sensitivity domain

Leif H. Cox
TechnoImaging, LLC
leif@technoimaging.com

Michael S. Zhdanov
U of Utah and TechnoImaging, LLC
mzhdanov@technoimaging.com

SUMMARY

We have developed a methodology to simultaneously invert large-scale airborne electromagnetic (AEM) survey data for conductivity and chargeability. The method is fully three-dimensional and includes full physics accounting for induced polarization and conductivity. The full dimensionality allows for the inclusion of inline, vertical, and cross-line components of the EM field in the inversion. This reduces non-uniqueness in the inverse models and avoids distortions due to 1D approximations. Accounting for the chargeability increases the accuracy of the recovered conductivity and allows for an additional physical parameter to aid in interpretation. The computer implementation of the method is based on the moving sensitivity domain approach, which enables the user to invert the large-scale geophysical survey data without losing resolution. The method has been used to interpret a large variety of AEM data acquired by different modern airborne systems. We demonstrate the efficacy of the developed technique of simultaneous 3D inversion of AEM data in two case studies using VTEM and TEMPEST data.

Keywords: 3D inversion, Airborne EM, Induced polarization, Moving sensitivity domain

INTRODUCTION

Modern airborne surveys collect thousands of lines of high-quality, multi-component electromagnetic (EM) data. Detailed analysis of these data is required to extract maximum value from the AEM surveys. Only multi-dimensional modeling and inversion can honour all components of the data simultaneously. This is crucial for geological interpretation.

Until recently, airborne EM (AEM) data have been inverted only for electrical conductivity. Detection of the IP effect using inductive sources and receivers was observed long ago and has generated interest in studying this phenomenon in airborne EM data. Early work by Smith and Klein (1996) demonstrated the feasibility of recovering IP parameters from airborne data. Goold et al. (2007) presented the first 3D method of simultaneous inversion of the AEM data into conductivity and changeability models. Veizzoli et al. (2020) used traditional 1D layered-earth approximations to further explore airborne IP with the Cole-Cole model. Kang et al. (2015) used the Cole-Cole model and 3D inversion to recover IP parameters, but the chargeability and conductivity were assumed to be decoupled in their inversion scheme. This paper demonstrates a more comprehensive method that allows full 3D inversion of large-scale AEM survey data for electrical conductivity and IP parameters, thereby improving interpretation and accuracy.

We use a moving sensitivity domain approach (Cox and Zhdanov, 2008; Cox et al., 2010; Zhdanov, 2018) with a variety of drivers (Cox et al., 2015) to reconstruct the electrical resistivity and chargeability of the earth. We demonstrate our technique by inverting the VTEM data from the Echum Area, Canada, and we revisit a TEMPEST survey from the Musgraves area of Australia, which has been extensively studied previously using a variety of AEM inversion techniques (Ley-Cooper et al., 2015).

METHODS

We will summarize our methods following the publications of Cox et al. (2024) and Cox et al. (2023).

Chargeability Model

For 1D inversion and 3D inversion, modeling is performed in the frequency domain. The fields are then transformed to the time domain using a cosine transform. This method allows for the incorporation of flexible IP parameterization within the modeling and inversion processes. The simplified GEMTIP model (Zhdanov, 2008), which is similar to the Cole-Cole model, is employed to parameterize the induced polarization effects:

$$\sigma(\omega) = \sigma\left(1 + \eta\left(1 - \frac{1}{1 + (i\omega\tau)^C}\right)\right), \quad (1)$$

where σ is the DC conductivity (S/m), ω is the angular frequency (rad/s), τ is the time constant, η is the intrinsic chargeability, and C is the dimensionless relaxation parameter. The dimensionless intrinsic changeability, η, characterizes the intensity of the IP effect.

Modeling and Inversion Methods

The workflow starts by completing the 1D inversion of the entire dataset and then using this for the background, starting, and reference models for the 3D inversion. The 1D modelling is performed in the frequency domain with a layered earth recursion factor and a fast Hankel transform (Nabighian, 1988). These results are then transformed to the time domain with a cosine transform and then convolved with the instrument's waveform. Sensitivities for the conductivity are found through perturbation, and then the sensitivities with respect to the rest of the GEMTIP parameters (τ, η, C) are found using the chain rule. Three-dimensional modeling is completed with either a contraction integral equation (CIE) (Zhdanov 2015, 2018) or a finite difference (FD) scheme (Cox et al., 2024). Both modelling techniques have advantages and disadvantages, and the choice can be made depending on the geology. Sensitivities for the CIE technique are found using the extended Born method, and sensitivities for the FD technique are found using reciprocity. The 3D inversions, both the CIE and FD versions, are calculated with the moving sensitivity domain approach (Cox and Zhdanov, 2008; Cox et al., 2010) to reduce memory and time requirements.

The inversion minimizes the parametric functional (Zhdanov, 2015):

$$P(\boldsymbol{m}) = \|\boldsymbol{W}_d(\boldsymbol{A}(\boldsymbol{m}) - \boldsymbol{d})\|^2 + \alpha\left\|\boldsymbol{W}_m\boldsymbol{L}(\boldsymbol{m} - \boldsymbol{m}_{apr})\right\|^2. \quad (2)$$

The data weights ($\boldsymbol{W}_d$) are based on the inverse of the estimated errors in the data and the model weights ($\boldsymbol{W}_m$) are based on the integrated sensitivities. Commonly referred to as a "depth weighting" term, the model weights attempt to equalize the sensitivities to all model parameters. The term $\boldsymbol{L}$ can be a roughening matrix to provide smoothness constraints or focusing matrices to provide a focused solution. In the case of induced polarization inversion, the model weights become very important to calculate rigorously because the data have widely varying sensitivities to the four GEMTIP model parameters, and the less important model parameters would not be adjusted without the corresponding model weight.

RESULTS

We illustrate the developed methods with two examples: 1) application to Geotech's VTEM system data; and 2) inversion of CGG's TEMPEST system data (currently operated by Xcalibur).

The VTEM airborne survey was conducted in February 2021 in Ontario, Canada, utilizing the full receiver waveform streamed data recording. The VTEM system operated at a 64 m terrain clearance and was concentric, with the X (inline) and Z (vertical) receivers positioned near the centre of and in the same plane as the 26 m diameter horizontal transmitter loop. The inversion process incorporated both X and Z components and used data from 42 µs to 8 ms.

The investigation focuses on the Wawa Greenstone Belt within the Echum project area (Cox et al., 2023). The geology of the region consists of 2.89 to 2.70-billion-year-old Precambrian rock, starting northeast of Lake Superior and extending to the western edge of the Kapuskasing Horst structural zone. The area features mafic to ultramafic bodies intruding into the metavolcanic-metasedimentary belt. Economically significant mineralization includes gold, silver, zinc, copper, and iron. Additionally, diamondiferous kimberlites and lamproites are found in the southeastern part of the Wawa Greenstone Belt, with gold deposits located around the northwest periphery of a granite-granodiorite batholith on the east side of the property. The project's primary objective was to locate disseminated sulphides and alteration zones, which were anticipated to be indicated by moderate conductivity or chargeability.

Figure 1 presents a horizontal slice of chargeability in part of the survey. The image shows a chargeability anomaly in an area of a conductivity anomaly. This location of the chargeability anomaly is geologically reasonable for alteration or sulfidation and is a possible mineralized zone. The inversion for chargeability in this survey provided more information from the data than inverting for conductivity alone. Additionally, the data could not be properly inverted without considering chargeability in the inversion (Cox et al., 2023), i.e., a reasonable conductivity model could not be recovered without accompanying chargeability.

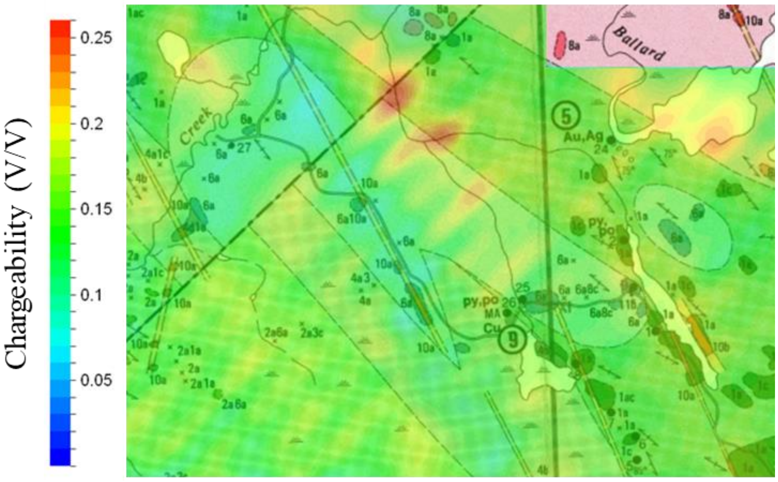

Figure 1. Chargeability slice at 150 m below the surface of the earth. Three chargeability highs can be seen, which are related to a major NE-SW trending fault and a geologic contact.

The second example is from a test line of TEMPEST data flown in South Australia. Three TEMPEST lines were flown as tests in 2016 in the Musgraves Region. One of these lines is from the survey that Geotech flew with their VTEM system. This was examined in great detail by Ley-Copper et al. (2014). The TEMPEST survey was flown at a transmitter height of about 120 m, with the receiver 115 m behind and 47 m below the transmitter. A 25 Hz 50% duty cycle transmitter waveform with a dipole moment of 288,000 NAI Am^2 was used. The acquired data were processed to a 100% duty cycle wave with B-field measurements and delivered at fifteen time channels from 13 µs to 16.2 ms of B_x and B_z data.

Figure 2 shows observed and predicted B_x TEMPEST data produced by the inverse model along a portion of Line 9000102. The anomaly at 7098500 mN is a conductive anomaly of interest. The data are fit relatively well, considering the noise floor set at 0.01 fT/Am^2.

Figure 3 presents the recovered conductivity structure along the line. Note that this is a single-line data, so the 3D inversion is highly constrained in the cross-line direction with the stabilizer. This allows us to run inversion on the single-line data, but 3D features are still recovered if they are required to fit the data. The anomaly at 709500 mN has a conductivity of around 1 S/m and a depth of around 150-200 m below the surface. This is shallower by 100-150 m than imaged by the methods in Ley-Cooper et al. (2014). It is common for 1D inversions to overdeepen anomalies. Plate modeling on this dataset also suggests a depth to the top of around 150 m, which corresponds to the result of 3D inversion.

Figure 4 shows chargeability recovered along the line from the airborne inversion. The chargeability is shown in the near-surface in the resistive center area of the line.

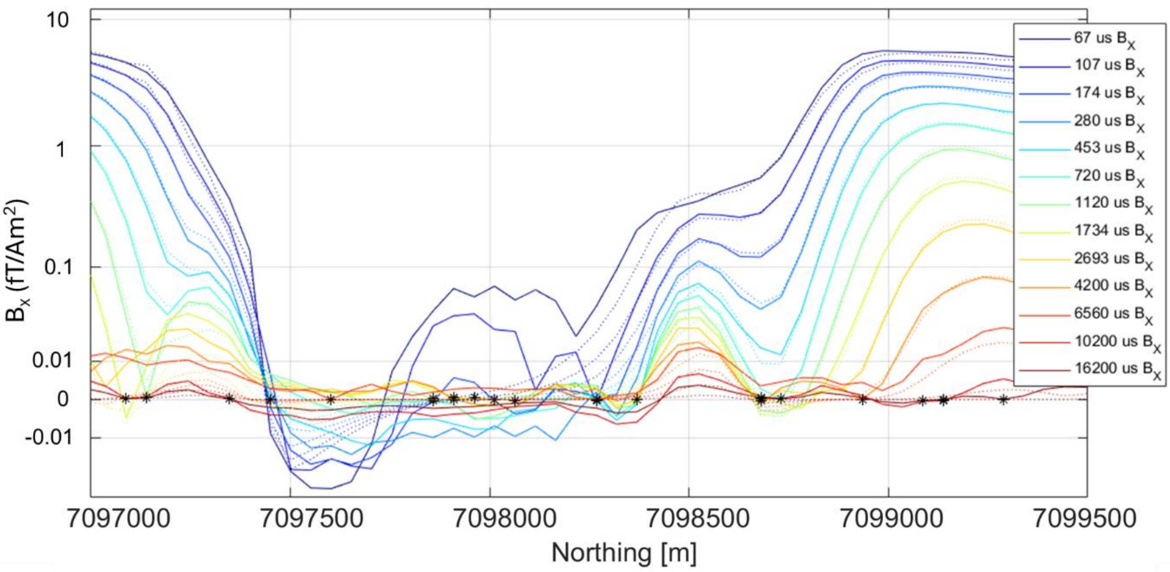

Figure 2. Observed (solid) and predicted (dotted) data along line L9000102 computed for the B_x component.

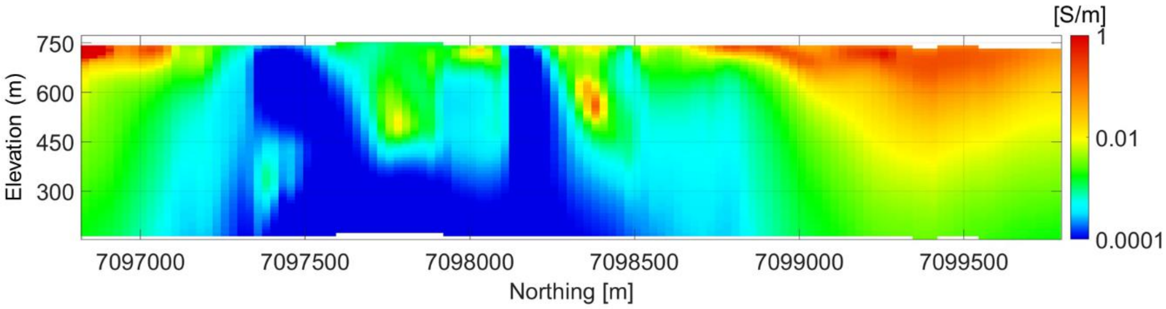

Figure 3. Vertical section of 3D inverse conductivity model under line L9000102.

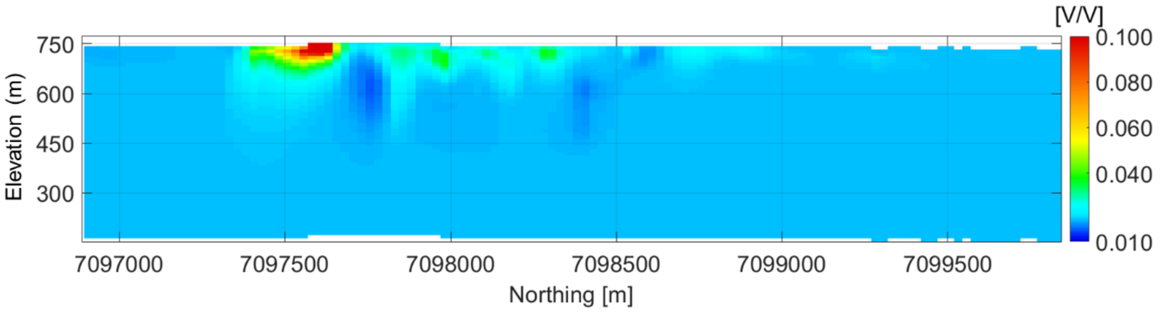

Figure 4. Vertical section of 3D inverse chargeability model under line L9000102.

CONCLUSION

We have developed a methodology and computer software to perform 3D inversions of large-scale airborne survey data. The advantages of 3D inversion over the traditional 1D layered earth inversion are two-fold:

1) The full dimensionality and true geometry of the earth is used in the modeling so three-dimensional effects are fully accounted for. With one-dimensional inversion, one assumes that the earth is comprised of infinite laterally invariant layers. Dipping structures and lateral variations are not modelled properly.

2) Because of the full dimensionality, both vertical and horizontal components (Z, X, and Y) of the airborne data are simultanoesouly included in recovering the conductivity structure of the earth. In the case of 1D inversion, the horizontal component data must be discarded with small ofset transmitter-reciever geometries.

The developed 3D inversion considers the presence of the IP effects in the airborne data and inverts the data to 3D conductivity and chargeability models. Including proper model weights is crucial to recovering resonable models. Ignoring the IP effect in airborne data may distort conductivity models dramatically. In addition, extracting IP information from AEM data is beneficial for geologic mapping and can lead to direct targeting in mineral exploration.

The 3D inversion algorithms employ the concept of moving sensitivity domain, allowing for the inversion of large AEM surveys without subdividing them into smaller pieces and without losing resolution. The developed methods have successfully applied to 3D inversion of the AEM data collected by all modern airborne EM systems, including the VTEM and TEMPEST shown here.

ACKNOWLEDGMENTS

The authors acknowledge TechnoImaging LLC and CEMI, University of Utah, for supporting this research. We are also grateful to Dr. Tim Munday of CSIRO for providing the field data.

REFERENCES

Cox, L. H., and Zhdanov, M. S., 2008, Advanced computational methods of rapid and rigorous 3-D inversion of airborne electromagnetic data: Communications in Computational Physics, 3 (1), 160-179.

Cox, L.H., Wilson, G.A. and Zhdanov, M.S., 2010. 3D inversion of airborne electromagnetic data using a moving footprint. Exploration Geophysics, 41(4), pp.250-259.

Cox, L., Endo, M. and Zhdanov, M., 2015, June. 3D Inversion of AEM Data Based on a Hybrid IE-FE Method and the Moving Sensitivity Domain Approach with a Direct Solver. In 77th EAGE Conference and Exhibition 2015 (Vol. 2015, No. 1, pp. 1-5). European Association of Geoscientists & Engineers.

Cox, L.H., Zhdanov, M.S. and Prikhodko, A., 2024. Inversion for 3D Conductivity and Chargeability Models Using EM Data Acquired by the New Airborne TargetEM System in Ontario, Canada. Minerals, 14(3), p.237.

Cox, L.H., Zhdanov, M.S., Pitcher, D.H. and Niemi, J., 2023. Three-dimensional inversion of induced polarization effects in airborne time domain electromagnetic data using the GEMTIP model. Minerals, 13(6), p.779.

Goold, J.W.; Cox, L.H.; Zhdanov, M.S., 2007, Spectral complex conductivity inversion of airborne electromagnetic data. In Proceedings of the SEG Technical Program Expanded Abstracts, San Antonio, TX, USA, 23–28 September 2007; pp. 487–491.

Kang, S. and Oldenburg, D.W., 2015. Recovering IP information in airborne-time domain electromagnetic data. ASEG Extended Abstracts, 2015(1), pp.1-4.

Ley-Cooper, A.Y., Viezzoli, A., Guillemoteau, J., Vignoli, G., Macnae, J., Cox, L. and Munday, T., 2015. Airborne electromagnetic modeling options and their consequences in target definition. Exploration Geophysics, 46(1), pp.74-84.

Nabighian, M.N. Electromagnetic Methods in Applied Geophysics: Voume 1, Theory; Society of Exploration Geophysicists: Houston, TX, USA, 1988; ISBN 0-931830-51-6.

Viezzoli, A. and Manca, G., 2020. On airborne IP effects in standard AEM systems: tightening model space with data space. Exploration Geophysics, 51(1), pp.155-169.

Smith, R.S. and Klein, J., 1996. A special circumstance of airborne induced-polarization measurements. Geophysics, 61(1), pp.66-73.

Zhdanov, M., 2008. Generalized effective-medium theory of induced polarization. Geophysics, 73(5), pp.F197-F211.

Zhdanov, MS, 2015. Inverse theory and applications in geophysics (Vol. 36). Elsevier.

Zhdanov, M. S., 2018, Foundations of geophysical electromagnetic theory and methods: Elsevier.